Refrigeration via purification through repeated measurements

Tanoy Kanti Konar, Srijon Ghosh, and Aditi Sen(De)
Harish-Chandra Research Institute, A CI of Homi Bhabha National Institute, Chhatnag Road, Jhunsi, Prayagraj 211019, India

(Received 6 June 2022; accepted 3 August 2022; published 29 August 2022)

We design a measurement-based quantum refrigerator with an arbitrary number of qubits situated in a one-dimensional array that interact through variable-range XY interactions. The method proposed is based on repeated evolution followed by a measurement on the single accessible qubit, which has the potential to reduce the temperature in the rest of the subsystems, thereby demonstrating cooling in the device. The performance of the refrigerator is quantified by the fidelity of each local subsystem with the ground state of the local Hamiltonian and the corresponding probability of success. We identify system parameters, which include the interaction strength, range of interactions, initial temperature of each qubit, and the position of the measured qubit, so that the fidelities of all the unmeasured qubits approach unity with a nonvanishing probability. We observe that although strong interactions during evolution are required to achieve cooling, the long-range interactions typically deteriorate the performance of the refrigerator, which indicates that interactions are not ubiquitous. We report the scalability and the saturation property of the success probability with respect to the system size, which turns out to be independent of the involved system parameters and the number of repeated measurements. Furthermore, we show that the number of subsystems which can be cooled changes depending on the odd or even number of sites in the refrigerator. We argue that the distribution of entanglement between unmeasured qubits can give a possible explanation of the dependence of cooling process on the measured and unmeasured sites.

DOI: 10.1103/PhysRevA.106.022616

I. INTRODUCTION

In the last few years, the breakneck modernization of technology has created several essential and pertinent directions in the field of quantum thermodynamics [1–4]. Rapid developments also demand designing quantum devices which perform more efficiently than the existing ones and can be built by using currently available technologies. In all discovered thermal machines, such as quantum batteries [5], quantum transistors [6], diodes [7], and quantum refrigerators [8–11], significant enhancements can be shown to be achieved in the quantum domain compared to classically available devices. Most importantly, these machines designed using the Dicke system [12], low- and higher-dimensional systems [13–16], mechanical resonators [17], and quantum spin models [11,18] have successfully been engineered in physically realizable substrates like cold atoms [19], nuclear magnetic resonances [20], trapped ions [21], atom-cavity systems [22], and superconducting circuits [23]. In spite of all these advancements, it has also been realized that there are several avenues through which the efficiencies of these devices can be improved.

Three interacting quantum systems [8,18,24–26], each connected to a noninteracting Markovian thermal bath with a different temperature, are a possible setup for a small quantum refrigerator. Typically, to lower the temperature of the *target system*, the dynamics of the system is controlled in such a manner that thermal energy is transferred to the hot bath from a cold one with the help of another heat bath, known as a *work reservoir* [27], both in the steady state and in the transient regimes. Precisely, the main aim of such a function of a refrigerator is to keep the state of the target system in the available ground state, so that the local temperature of the system becomes the minimum, thereby achieving the cooling. Numerous works were recently carried out in this direction, concentrating mainly on systems consisting of qubits, qubit-qutrit systems [8,28,29], and also higher-dimensional spin systems [16]. In addition, these steady-state cooling procedures can be accomplished with external energy sources or by disallowing sources of external control, thereby leading to self-contained heat engines [8,30] or in a periodically driven system [31] or via repeated collision [32] or with a reverse-coupling mechanism [33].

All the aforementioned designs of quantum refrigerators are restricted by the fact that the state of the target system can attain the corresponding ground state from an arbitrary thermal state, thereby arriving at a temperature lower than its initial one by means of the open-system evolution described by the Gorini-Kossakowski-Sudarshan-Lindblad master equation [27,34]. In this work, we choose a completely distinct route: Starting from the local spin Hamiltonian, the phenomenon of cooling, i.e., the refrigeration of several quantum systems, is achieved via repeated unitary evolution of the entire system governed by quantum prototypical spin models followed by a measurement on a single accessible qubit. From a different perspective, the repeated-measurement scenario was first considered in the context of purifying a subsystem from the mixed state by performing frequent measurements on another subsystem [35,36]. Almost at the same time, a unitary evolution-based cooling protocol of a nearest-neighbor spin system was proposed [37,38] in which by using a set of noninteracting qubits (controller system), the sequential

interactions between one of the controllers and the spin model lead to cooling by applying a unitary SWAP operator. It was later used to cool a mechanical resonator by performing measurements on the flux qubits which are in contact with the resonator [17,39–41] and also in spin systems [42]. Recent work generalized the situation for double resonators, thereby achieving simultaneous cooling [43,44]. It was also shown that in this process of repeated measurements, bipartite as well as multipartite entangled states can be generated [35,36,45,46].

In this proposal, the state of the measured qubit is initially taken to be the ground state of the local Hamiltonian, while unmeasured qubits are prepared in the thermal state of the same local Hamiltonians. At a later time, the interactions between measured and unmeasured qubits are turned on according to the anisotropic variable-range XY Hamiltonian up to a certain interval of time to generate the correlation between the systems. We now address the following question: Is it possible to refrigerate every individual unmeasured qubit of the system by measuring only a particular subsystem repeatedly? We answer it affirmatively. We report that by choosing the system parameters, the time of evolution, and the measurement basis appropriately, it is possible to decrease the temperature of every individual qubit with a finite probability when the dynamics is governed by both short- and long-range interactions. In particular, a successful cooling process is measured by computing the fidelity between the time-evolved reduced subsystem after measurements and the corresponding ground state of each local subsystem. Notice that the procedure of cooling is different from the quantum Zeno effect [47], which deals with frequent measurement, thereby slowing down the dynamics of the system.

When a refrigerator consists of three spin-$\frac{1}{2}$ particles, we derive analytical forms of fidelity after arbitrary rounds of evolution and measurements. Numerical simulations reveal that when a one-dimensional (1D) array of spins composed of at most eight spin-$\frac{1}{2}$ particles represents a refrigerator, the fidelity depends crucially on the range of interactions, system parameters, and position of the measured qubits in the array. Although the protocol is probabilistic, we find that the probability of successfully achieving cooling saturates to a finite nonvanishing value with the number of measurements, and we also report its scaling with the system size when cooling occurs for all the unmeasured qubits which are independent of the system parameters.

Some previous works [35,36] showed that one can generate a multiparty entangled state by measuring on a single qubit repeatedly. We show here that the cooling procedure can be connected to the distribution of entanglement [48,49] among unmeasured qubits. In particular, a decrease in the sum of entanglement between the unmeasured qubits immediately implies that the refrigerator works. This is due to the fact that quantum correlation created in the initial steps induces cooling in the system, although the procedure becomes successful only when the final state produced between unmeasured qubits is a fully separable state.

This paper is organized as follows: In Sec. II, we introduce the model of refrigeration for an arbitrary number of qubits interacting through the variable-range interaction and define the figure of merit. In Sec. III, we derive a compact analytical form of fidelity for a three-qubit refrigerator and compare the performance depending on the position of the measured qubits. Proceeding further in Sec. IV, we examine the effects of measurements and coupling strength when the initial states of the subsystems are maximally mixed for a refrigerator built with more than three spin-$\frac{1}{2}$ particles. Section IV B reports the efficiencies of the refrigerator when the unmeasured qubits are prepared in the thermal state with moderate temperature. In Sec. V, we present the consequences of measurements performed on different spatial positions on cooling, and we finally conclude in Sec. VI.

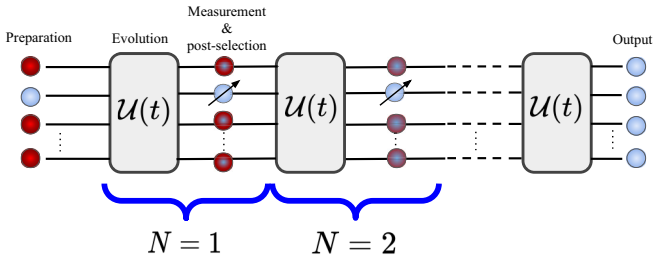

FIG. 1. Steps of a measurement-based refrigerator. An arbitrary qubit (blue) which is initially prepared as the ground state of the local Hamiltonian is chosen for the measurement, while the rest of the qubits (red) are initially in the thermal state of a local Hamiltonian with finite temperature. The system evolves according to the unitary operator $\mathcal{U}(t)$ followed by a measurement on a single qubit which is in the ground state. By properly choosing the desired output state of the measured qubit, we again let the whole system evolve according to the same unitary. The aim of such repeated evolutions followed by measurements is to project all (some) of the qubits to the ground state of the local Hamiltonian, thereby achieving cooling. We show that it is indeed possible to achieve.

II. REPEATED MEASUREMENT-BASED REFRIGERATOR MODEL

Let us first introduce the setup of a refrigerator based on repetitive quantum measurements (Fig. 1). The model consists of L spin-$\frac{1}{2}$ particles, denoted as $A_1, A_2, \ldots, A_L$, governed by the local Hamiltonian H_{A_i} $(i = 1, 2, \ldots, L)$ in a one-dimensional array, as depicted in Fig. 2. The measurement is performed on a single accessible qubit placed in any arbitrary position of the array, referred to as A_j^M $(j \neq i)$, which is prepared in the ground state $|\mathcal{G}_{A_j^M}\rangle$ of its local Hamiltonian $H_{A_j^M}$. The rest of the unmeasured qubits are prepared in the thermal states of their respective local Hamiltonians H_{A_i} $(i = 1, 2, \ldots, L,\ i \neq j)$. Hence, the initial state of the total L-party system reads

$$\rho(0) = |\mathcal{G}_{A_j^M}\rangle\langle\mathcal{G}_{A_j^M}| \otimes \rho_{\text{in}}^{L-1}, \tag{1}$$

where $\rho_{\text{in}} = \bigotimes_{i\neq j,i=1}^{L} \rho_{A_i}$ is the initial state of the unmeasured qubits. Notice that the initial state is fully separable, having vanishing multiparticle as well as bipartite entanglement [50–52]. When $t > 0$, the system evolves according to the Hamiltonian H_{ev}, consisting of $\sum_i H_{A_i} + H_{A_j^M} + H_{\text{int}}$ for a certain interval of time t, where H_{int} represents the interaction term between L spin-$\frac{1}{2}$ particles (see Fig. 2). In this situation,

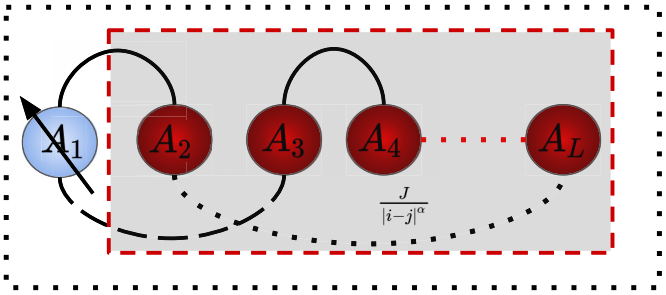

FIG. 2. Schematic diagram of the spin-chain where during dynamics, the system evolves according to $H_{\rm ev}$, containing the variable-range interacting Hamiltonian $H_{\rm int}$, which scales as $\frac{J}{|i-j|^\alpha}$, with i and j being the sites of the spins. An accessible qubit is chosen for the measurement and is initially prepared as the ground state of the local Hamiltonian, while the rest of the inaccessible qubits (shaded region) are initially in the thermal state with finite temperature.

it is reasonable to expect that the corresponding global unitary operator, $\mathcal{U}(t) = \exp(-iH_{\rm ev}t)$, is responsible for creating quantum correlation between L subsystems. The evolution is followed by an arbitrary projective measurement at site A_j^M with the set of projection operators $\{\Pi_k^M\}_{k=1}^2$, whose elements are the ground and excited states of $H_{A_j^M}$. Postselection of the output state is performed to ensure that the measured qubit A_j^M is projected to the ground state, i.e., $\Pi_1^M = |\mathcal{G}_{A_j^M}\rangle\langle\mathcal{G}_{A_j^M}|$, and we discard the process if the excited state clicks and start the protocol from the beginning. In the case of the desired outcome, Π_1^M, the entire process is repeated an arbitrary number of times, say, N times, until the individual $L-1$ qubits reach their respective ground states of the initial Hamiltonian $|\mathcal{G}_{A_i}\rangle$. Starting from a thermal state with an arbitrary high temperature, the above process demonstrates that repeated evolution for a short period of time and projective measurements can drive all (some of) the unmeasured subsystems to reach the ground states, thereby lowering the temperature (energy) of the individual subsystem as well as the entire system. We call this procedure refrigeration. In other words, cooling occurs successfully when purification of thermal states takes place, thereby reaching pure states with minimum energy. Note that in contrast to the well-known Zeno measurement, we consider the time of the dynamics t to be nonvanishing and finite and the repetition of measurements N to be large but finite. As argued in Ref. [35], purification of the unmeasured part of the system occurs due to the projection into the eigenstate corresponding to the maximum eigenvalue of the nonunitary evolution operator. With an increasing number of measurements, such an eigenstate dominates depending on the choice of parameter, and hence, we can project an unmeasured state to a different purified state by tuning system parameters suitably. This picture is similar to the above-proposed protocol in which changing the spatial position of the measurement can lead to different eigenstates of the nonunitary evolution, thereby leading to distinct fidelities of the unmeasured qubits. We will also show that successful implementation of the cooling process can be explained via the entanglement properties of the unmeasured qubits.

After the completion of the whole process of repeated evolution and measurements for a particular interval of time t, the resultant state in the case of the desired outcome from the measurement can be represented as

$$\rho(t) = \frac{1}{p_N}\left(\Pi_1^M\mathcal{U}\right)^N\rho(0)\left(\Pi_1^M\mathcal{U}^\dagger\right)^N. \tag{2}$$

Here p_N is the probability of a successful implementation of cooling at each step, which can be calculated as

$$p_N = \mathrm{Tr}\left[\left(\Pi_1^M\mathcal{U}\right)^N\rho(0)\left(\Pi_1^M\mathcal{U}^\dagger\right)^N\right] \tag{3}$$

when the measurement outcome at each step is Π_1^M at site A_j^M. We calculate the reduced state of each unmeasured subsystem by tracing out the other $L-1$ qubits, given by

$$\rho_{A_i}(t) = \mathrm{Tr}_{\bar{A}_i}[\rho(t)], \tag{4}$$

where $\overline{A_i}$ represents all the qubits except A_i. As mentioned before, the main focus in building a refrigerator is to arrive at the ground state of as many unmeasured qubits as possible. To measure the performance of the refrigeration, we compute the fidelity of each qubit after an arbitrary step N in the ground state of the local Hamiltonian H_{A_i}, which mathematically reads

$$\mathcal{F} \equiv \mathcal{F}_{A_i}(N) = \langle\mathcal{G}_{A_i}|\rho_{A_i}(t)|\mathcal{G}_{A_i}\rangle, \tag{5}$$

where $|\mathcal{G}_{A_i}\rangle$ is the ground state of qubit A_i, corresponding to the initial Hamiltonian H_{A_i}. Note that $\mathcal{F}$ also depends on the tuning parameter of the system, which can be a function of different parameters involved in the system like the interaction strength, the range of interactions, the strength of the magnetic field, and the initial temperature of the unmeasured qubits. Since our aim is to build a proper refrigerator, we continue the process until the fidelities for all (some) of the qubits approach unity. Hence, during investigations, we have to choose suitable (optimized) system parameters as well as projection operators so that the cooling is achieved. Moreover, each step consists of measurements, and the performance of the refrigerator can be ensured only if one obtains a nonvanishing probability p_N after N steps for some subsystems.

Realizing refrigeration with quantum spin models

The refrigerator discussed above has three important components: (1) the initial state of the individual qubit governed by a local Hamiltonian; (2) the evolution operator, especially the interaction part, which is responsible for nontrivial dynamics; and (3) the projective measurement. Let us illustrate each ingredient of a refrigerator for a specific implementation considered in this paper.

Initial states. The initial state of $L-1$ unmeasured qubits is considered to be the thermal state of their local Hamiltonian,

$$H_{A_i} = \frac{\omega_{A_i}}{2}\sigma_i^z, \tag{6}$$

where σ_i^μ $(\mu = x, y, z)$ is the Pauli matrices acting on the subsystem i while the measured one is initially prepared as the ground state of the same Hamiltonian. Here ω_{A_i} is the strength of the external magnetic field on qubit A_i. Therefore, the initial

state reads

$$\rho_{\text{in}} = \bigotimes_{i\neq j} \frac{1}{\mathcal{Z}_i} \exp\big(-\beta H_{A_i}\big) \otimes \big|\mathcal{G}_{A_j^M}\big\rangle\big\langle\mathcal{G}_{A_j^M}\big|, \tag{7}$$

where $\beta = \frac{1}{k_B T}$ is the inverse temperature corresponding to the absolute temperature T, with k_B being the Boltzmann constant, and $\mathcal{Z}_i = \text{Tr}\,[\exp(-\beta H_{A_i})]$. We assume β is the same for all the unmeasured spins.

Evolution operator. The integral part of a refrigerator is the unitary evolution of the whole system for establishing the quantum correlation between the qubits, which plays an important role in achieving cooling. The unitary dynamics is dictated by the local Hamiltonian H_{A_i} $(i = 1, 2, \ldots, L)$ along with the interacting variable-range XY Hamiltonian,

$$H_{\text{int}} = \sum_{i<j}^{L} \frac{J_{ij}}{4}\big[(1+\gamma)\,\sigma_i^x\,\sigma_j^x + (1-\gamma)\sigma_i^y\sigma_j^y\big], \tag{8}$$

where γ is the anisotropy parameter in the xy plane; J_{ij} is the interaction strength between qubits i and j, which varies according to the variable-range interaction, $J_{ij} \sim \frac{J}{|i-j|^\alpha}$, with α being the falloff rate of the interaction strengths between different subsystems; and J is a coupling constant which dictates a ferromagnetic $(J < 0)$ or antiferromagnetic $(J > 0)$ type interaction between the qubits. Note that a large value of α, i.e., $\alpha > 2$, actually mimics the nearest-neighbor Hamiltonian, while $\alpha \leqslant 1$ mimics the long-range behavior. Therefore, the Hamiltonian which dictates the evolution can be written as $H_{\text{ev}} = \sum_i H_{A_i} + H_{\text{int}}$.

Measurements. Let us consider a linear array of spins in which projective measurements $\{\Pi_k^M = |\mathcal{G}_{A_j^M}\rangle, |\mathcal{E}_{A_j^M}\rangle\}$ is performed on the qubit A_j^M. In this scenario, $\{\Pi_k^M\}$ reduces to a measurement in the computational basis, i.e., $\{|0\rangle, |1\rangle\}$ at each step. We continue the process only when the outcome $|1\rangle$ which is the ground state of the local Hamiltonian in Eq. (6) clicks.

III. THREE-QUBIT MEASUREMENT-BASED REFRIGERATOR

Let us first illustrate the performance of a measurement-based refrigerator consisting of three spin-$\frac{1}{2}$ particles. Refrigerators built with a higher number of qubits will be dealt in the following section.

First qubit as the accessible one. Let us consider the scenario where the qubits are placed in a 1D array (as in Fig. 2) and the measured one is the first qubit A_1^M, while the rest of the qubits are denoted by A_2 and A_3. The initial state in this case is taken to be

$$\rho(0) = \big|\mathcal{G}_{A_1^m}\big\rangle\big\langle\mathcal{G}_{A_1^m}\big| \bigotimes_{i=2}^{3} \frac{1}{\mathcal{Z}_i}\big[\exp\big(-\beta H_{A_i}\big)\big], \tag{9}$$

where the unmeasured qubits are the thermal states of the local Hamiltonian in Eq. (6) and the measured qubit is the ground state of the same Hamiltonian. We will argue later that the spatial position of the measured qubit also affects the cooling mechanism. Notice that when the temperatures of the unmeasured initial states are below some critical temperature, the local states are close to the ground state of the local Hamiltonian H_{A_i}, thereby leading to a trivial situation. On the other hand, an interesting scenario emerges when the temperature of the initial state is high enough.

Let us start with an extreme case, i.e., when the unmeasured qubits are initially prepared as maximally mixed, i.e., the thermal states with $\beta = 0$. The system evolves according to the nearest-neighbor XX Hamiltonian in the presence of a magnetic field, given in Eqs. (8) and (6) with $\gamma = 0$, $\alpha > 2$, and $\omega_{A_i} = 1$, while the measurement on the qubit A_1^M is performed in the basis of the local Hamiltonian, i.e., $\{|\mathcal{G}_{A_1^M}\rangle, |\mathcal{E}_{A_1^M}\rangle\}$. All the qubits evolve for a short period of time t which is followed by a measurement. After N steps of the evolution and measurement, the resulting tripartite state can be found to be

$$\begin{aligned}\rho(t) = {} & x|100\rangle\langle 100| + yP[a|110\rangle + b|101\rangle] \\ & + (1-y-x)|111\rangle\langle 111|,\end{aligned} \tag{10}$$

where $|1\rangle$ and $|0\rangle$ represent the ground and excited states of H_{A_i}, respectively; x, y, a, and b depend on the system parameters as well as repetition of the process N; and P is the projector. When the outcome of the measurement is $|\mathcal{G}_{A_1^M}\rangle$, the output state at each subsystem $\rho_{A_i}^f$ turns out to be diagonal in the computational basis, given by

$$\rho_{A_i}^f = \frac{1}{\mathbb{N}}\big(\eta_{A_i}\big|\mathcal{G}_{A_i}\big\rangle\big\langle\mathcal{G}_{A_i}\big| + \eta'_{A_i}\big|\mathcal{E}_{A_i}\big\rangle\big\langle\mathcal{E}_{A_i}\big|\big). \tag{11}$$

Here $|\mathcal{E}_{A_i}\rangle$ denotes the excited state of the local Hamiltonian, the coefficients η_{A_i} and η'_{A_i} are functions of $\sum_{r=1,3,\ldots}^{2N-1} A_r \cos(\frac{Jtr}{\sqrt{2}})$ with only odd r and $\sum_{r=1}^{N} B_r \cos(\sqrt{2}Jtr)$ up to some constant factor, and $\mathbb{N}$ is the normalization constant. To quantify the performance of the refrigerator, the corresponding fidelity of qubit A_i $(i = 2, 3)$ can be represented as

$$\mathcal{F}_{A_i}(N) = \big\langle\mathcal{G}_{A_i}\big|\rho_{A_i}^f\big|\mathcal{G}_{A_i}\big\rangle, \tag{12}$$

which takes the following form, after N rounds:

$$\begin{aligned}\mathcal{F}_{A_i}(N) = \frac{1}{\mathbb{N}}\Bigg[& C_{A_i}^N + \sum_{r=1,3,\ldots}^{2N-1} C_{A_i}^{\prime r} \cos\left(\frac{Jrt}{\sqrt{2}}\right) \\ & + \sum_{r=1}^{N} C_{A_i}^{\prime\prime r} \cos(\sqrt{2}Jtr)\Bigg], \quad i = 2, 3.\end{aligned} \tag{13}$$

The coefficients $C_{A_i}^N$, $C_{A_i}^{\prime r}$, and $C_{A_i}^{\prime\prime r}$ depend on the number of times evolution and measurement operators N act on the system and other system parameters. After a few such steps, the fidelity gets close to unity, provided Jt is chosen appropriately. To visualize the dependence on parameters, we plot $\mathcal{F}_{A_2}$ and $\mathcal{F}_{A_3}$ by varying J for $N = 10$ and $t = 1$ in Fig. 3. Notice that the two-party reduced density matrix between the inaccessible qubits which is obtained after measuring on the first qubit is again a function of x, y, a, and b and the second term is responsible for generating entanglement in the system. We find that by increasing the number of measurements N the cross term vanishes, which leads to a fully separable state for their corresponding ground states (i.e., $\mathcal{F}_{A_i} = 1$), describing the phenomenon of cooling. Due to symmetry, a similar cool-

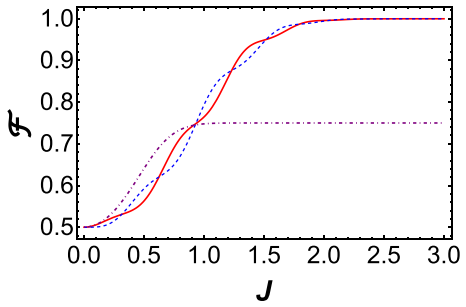

FIG. 3. Variation of the fidelity as a function of the interaction strength J. The refrigerator consists of three qubits which interact with each other via the nearest-neighbor XX Hamiltonian in the presence of magnetic field in Eq. (8) with $\alpha > 2.5$. The initial state is a fully separable state, given in Eq. (9) with $\beta = 0$. Dashed and solid lines represent the fidelities of the second and third qubits (ordinate) with respect to J (abscissa) when the measurement is performed in the first qubit. The dash-dotted line corresponds to $\mathcal{F}$ for the first and third qubits due to the symmetry with the measurement being done on the second qubit. Here $t = 1$, and $\omega_i^{A_i} = 1\ \forall i \in \{1, 2, 3\}$. Both axes are dimensionless.

ing phenomenon occurs when the measurement is performed on the third qubit.

Second qubit as the measured qubit. Suppose the measured qubit is the second one, i.e., the system is initially prepared as

$$\rho(0) = \frac{1}{\mathcal{Z}_1}\exp\big(-\beta H_{A_1}\big) \otimes \big|\mathcal{G}_{A_2^M}\big\rangle\big\langle\mathcal{G}_{A_2^M}\big| \otimes \frac{1}{\mathcal{Z}_3}\exp\big(-\beta H_{A_3}\big),$$

with $\beta = 0$. After evolving $\rho(0)$ via the XX Hamiltonian with a magnetic field H_{ev} and measuring the middle qubit in the $\{\Pi_k^M\}$ basis, we find that both the first and third qubits reach the same diagonal states when $|1\rangle$ clicks, which is in contrast to the previous situation. Since both the first and third qubits are nearest neighbors with the measured qubit, the system possesses a symmetry which finally leads to the same state at the first and third subsystems after N steps. In this case, after N repetitions, the output three-qubit state becomes

$$\begin{aligned}\rho(t) = x'|010\rangle\langle 010| + y'P[a'|110\rangle + b'|011\rangle] \\ + (1 - y' - x')|111\rangle\langle 111|,\end{aligned} \tag{14}$$

and the corresponding fidelity in any unmeasured subsystem is given by

$$\mathcal{F}(N) = \frac{4^{N-1}}{C^N + \sum_{r=1}^{N} C'^r \cos(\sqrt{2}Jtr)}, \tag{15}$$

where C^N and C'^r take values depending on the number of rounds of evolution and measurements being carried out. Comparing fidelities in Eqs. (14) and (15), we observe that fidelities depend on the spatial position of the unmeasured qubit with respect to the measured one. Unlike in the previous scenario, the entanglement-generating term in this case does not vanish with the increase of N. As a result, by measuring on the second qubit, we cannot achieve refrigeration since the joint state of the unmeasured qubits always remains entangled. Later, we will discuss the dependence of the spatial position of the measured qubit on the refrigeration in detail. Note, however, that the probability is higher for the case with nonunit fidelity than the one with unit fidelity.

IV. REFRIGERATION WITH AN ARBITRARY NUMBER OF SITES

We will now investigate the performance of a refrigerator which comprises an arbitrary number of qubits. We consider a setup in which all the unmeasured qubits are initially prepared at infinite temperature; that is, the states are maximally mixed, and the measured qubit is in the ground state of the corresponding Hamiltonian. Moreover, we ensure here that the spins are situated in a chain with an open boundary condition and the first or last qubit is chosen for measurement. Without loss of generality, the initial fully separable state of the total system reads

$$\rho(0) = \big|\mathcal{G}_{A_1^M}\big\rangle\big\langle\mathcal{G}_{A_1^M}\big| \bigotimes_{i=2}^{L}\left[\frac{1}{2}(|0\rangle\langle 0| + |1\rangle\langle 1|)\right]. \tag{16}$$

When $t > 0$, the interaction between the qubits is turned on, which allows the evolution of the total system according to $\mathcal{U}(t) = \exp(-iH_{\text{ev}}t)$. Our aim is to observe the final states of the unmeasured qubits after N rounds of projective measurements, where one of the elements can be represented as $\Pi_1 = |\mathcal{G}_{A_1^M}\rangle\langle\mathcal{G}_{A_1^M}| \bigotimes \mathbb{I}_{L-1} = |1\rangle\langle 1| \bigotimes \mathbb{I}_{L-1}$, with $\mathbb{I}_{L-1}$ being the identity operator of the unmeasured Hilbert space. The phenomenon of refrigeration demands a situation in which the states of all the unmeasured qubits are in the ground state of the respective Hamiltonian, i.e., in which the projection operator $|1\rangle$ clicks.

As we have shown in the case of three qubits in Fig. 3, the system parameters involved in the process play a crucial and delicate role in this cooling procedure. Let us first explain the choice of the system parameters which are relevant during the dynamics for successful implementation of a quantum refrigerator with an arbitrary number of sites. Numerical simulation is performed for a 1D array containing $L = 8$ sites.

Effect of interaction strength. Let us take the initial state in Eq. (16) and $H_{\text{ev}} = H_{A_i}(\omega_{A_i} = 1) + H_{\text{int}}(\gamma = 0)$. We also fix the number of repeated evolutions and measurements to be $N = 500$, and the time interval in which the evolution takes place is chosen to be unity. In this setup, we observe that the fidelity between the reduced subsystem A_i and the respective ground state of that particular qubit increases with the increase of interaction strength J, as depicted in Fig. 4 for different values of α, with $L = 8$. This implies that a reasonably high interaction strength is required for a successful implementation of a refrigerator. In addition, we observe that ferromagnetic or antiferromagnetic interactions do not play a role in the performance, which we can also understand from the expressions of fidelities obtained in Eqs. (14) and (15).

Moreover, for the nearest-neighbor Hamiltonian (i.e., when $\alpha = 2.5$), all the unmeasured qubits reach their corresponding ground state for a small value of J compared to the evolution governed by the long-range quantum spin models (i.e., $\alpha < 2$). Notice that the moderate values of $N \geqslant 100$, L, and $t \geqslant 1$ do not alter the results qualitatively. However, the presence of anisotropy in the dynamics typically has a detrimental effect on fidelity as well as probability, thereby establishing that the

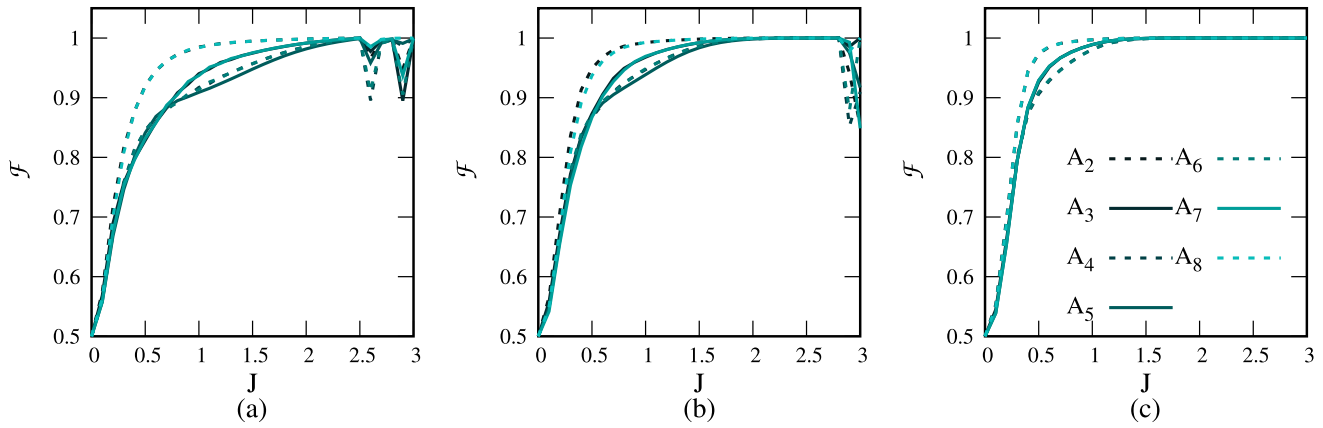

FIG. 4. Fidelity (ordinate) vs the interaction strength between qubits J (abscissa) for different values of α. Here (a), (b), and (c) correspond to $\alpha = 1.0, 1.5$, and 2.5, respectively. The initial state is given in Eq. (16) with $\beta = 0$, and the evolution Hamiltonian contains both the interacting Hamiltonian in Eq. (8) with $\gamma = 0$ and the local Hamiltonian H_{A_i} in Eq. (6). A_i's represent the unmeasured qubits while the measurement is performed on the first (last) qubit of the chain and the outcome of the measurement is the ground state of the local Hamiltonian. Dashed (solid) lines represent even (odd) positions of the qubits. In both cases, the shade goes from dark to lighter with the increasing value of the position of the qubits. System size is taken as $L = 8$. Here $N = 500$, and $\omega_i^{A_i} = 1\ \forall\, i \in \{1, \ldots, 8\}$. All the axes are dimensionless.

XX interacting Hamiltonian leads to the best performance in cooling.

Interestingly, the fidelity of the subsystem follows a particular pattern with J in a spin chain of length L. If the measurement is carried out on the first qubit, the qubits $(k+1)$ and $(L-k+1)$ for a chain with even L $[k = 1, 2, 3, \ldots (\frac{L}{2} - 1)]$ and $[k = 1, 2, \ldots, \lfloor \frac{L}{2} \rfloor]$ for odd L reach the maximum fidelity simultaneously with J for a fixed N. This is due to the inherent parity symmetry present in the system even when the open boundary condition is taken. Strikingly, the qubits farthest from and nearest to the measured one reach unit fidelity with a smaller number of repeated measurements N compared to all the other qubits located in the middle of the spin chain, which require high values of N and interaction strength to achieve the same result.

Dependence on the number of measurements. To investigate the number of steps required to cool down the subsystem of a spin chain of length L, we fix the other parameters. It is important to stress here that although some specific parameters are chosen for presenting the results, it is possible to identify the parameter regime where the cooling phenomenon can be found (as shown in Fig. 4). We have already realized that successful realization of a refrigerator depends on a strong interaction strength in the dynamics, and hence for demonstration, we choose $J = 3$, $\omega_{A_i} = 1$, $t = 1$, and $L = 8$. The results presented here remain unaltered for other system parameters such as $J > 3$ and $t > 1$ starting with the same initial state in Eq. (16). Moreover, we tune the falloff rate of interactions between the qubits so that we can generate the effects of nearest-neighbor as well as long-range interactions on fidelities. Let us summarize the observations.

(1) After evolution and measurements as per the prescription, we find that all the unmeasured qubits can be projected to their ground state for different values of variable-range interaction strength (see Fig. 5). Notice that in Fig. 5, the choice of J turns out to be suitable for $\alpha = 1$ and $\alpha = 2.5$,

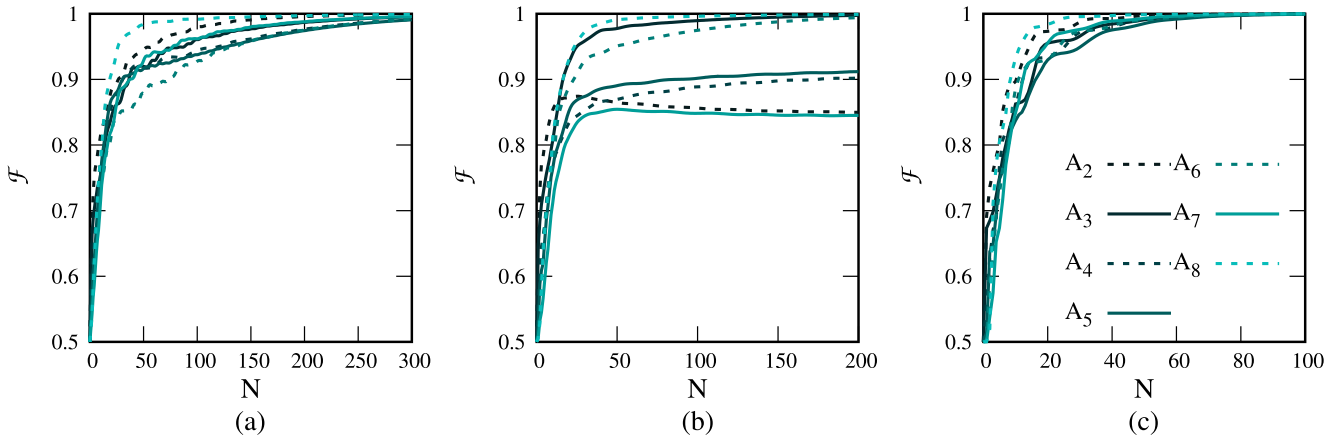

FIG. 5. Fidelity (vertical axis) with respect to the number of rounds N (horizontal axis). Here the interaction strength $J = 3$. All other specifications are the same as in Fig. 4. All axes are dimensionless.

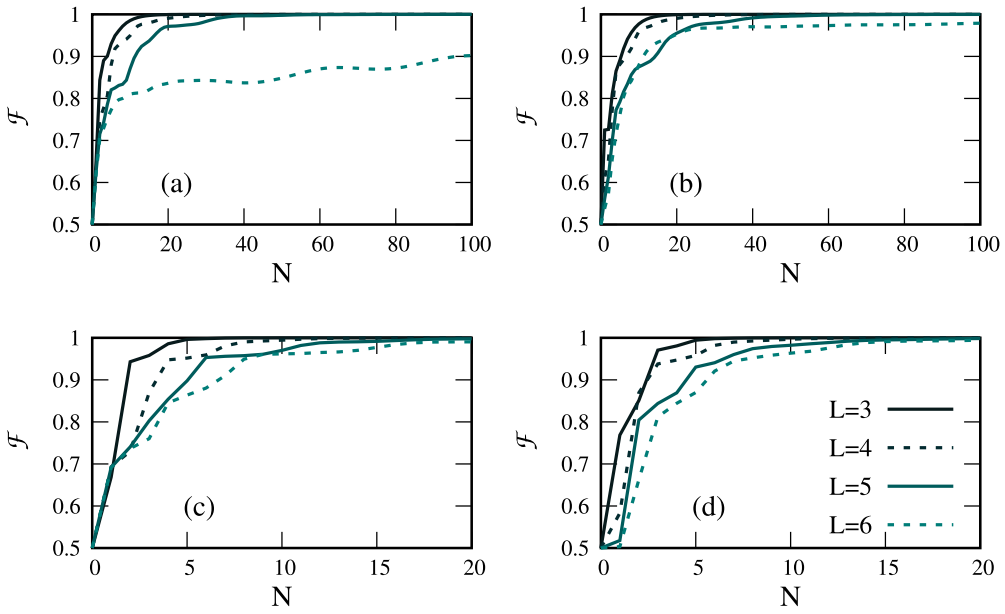

FIG. 6. Fidelity (ordinate) as a function of the number of measurements N (abscissa) for different system sizes L. We study the dependence of the fidelity of the unmeasured qubit adjacent to the measured qubit and the qubit situated farthest from the measured one. Solid and dashed lines represent odd and even lattice sites, respectively. The other parameters of the systems are $J = 3$ and (a) and (b) $\alpha = 1$ or (c) and (d) $\alpha = 2.5$. (a) and (c) correspond to the fidelity for the qubit adjacent to a measured qubit, i.e., the second qubit since the measurement is carried out on the first qubit, while (b) and (d) represent the behavior of $\mathcal{F}$ for the farthest qubit, i.e., the qubit in the boundary A_i ($i = 3, \ldots, 6$). All other specifications are the same as in Fig. 4. All the axes are dimensionless.

although it is not appropriate for $\alpha = 1.5$, and hence, there are qubits which do not approach the unit fidelity. However, proper tuning of J can also cause the fidelities of all the qubits to go to unity even for $\alpha = 1.5$, as seen in Fig. 4.

(2) An interesting question can be addressed at this point: Does the distance of a qubit from the measured one matter to achieve the maximum fidelity of a qubit? More specifically, we figure out the position of the qubit that reaches the maximum fidelity with minimum N. We observe that irrespective of α, the qubit most distant from the measured qubit goes to the ground state with the minimum number of measurements compared with other qubits present in the system. However, N required for other unmeasured qubits do not follow any hierarchy based on the distance from the measured qubit.

Scalability: Role of system size. Let us address here the scalability of the machine. In other words, when we increase the system size and measure only on a single qubit repeatedly, we investigate the scaling of fidelity with L. Since the number of subsystems to be cooled increases with L, we notice that the number of measurements required for cooling also increases with L, as shown in Fig. 6 for two different values of α. Moreover, we observe that for a fixed L with high values of α, i.e., when the interaction strength is confined between the nearest pair of qubits, it is possible to decrease the temperature of all the qubits much more efficiently than in the model with long-range interactions [compare Figs. 6(a) and 6(b) with 6(c) and 6(d)].

When the number of measurements is low enough, there is no prominent pattern of fidelity with system size. However, for moderate values of N, a clear pattern with increasing system size emerges, as depicted in Fig. 6.

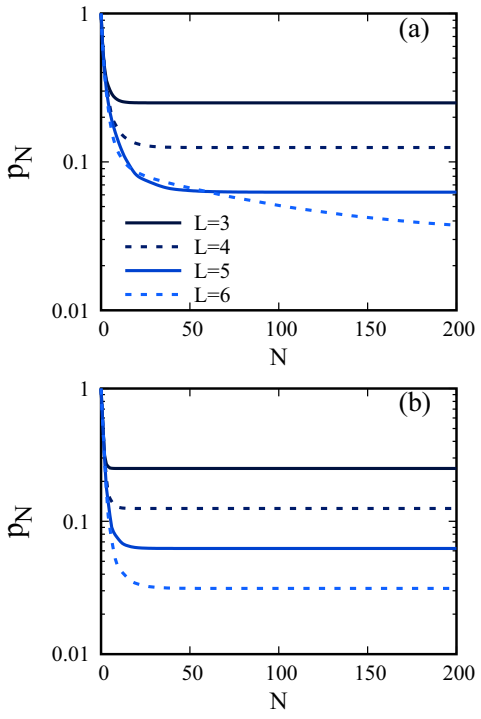

FIG. 7. Probability p in log scale (y axis) vs N (x axis) for different system sizes. (a) $\alpha = 1$ and (b) $\alpha = 2.5$. Here $J = 3$ in H_{ev}. All other specifications are the same as in Fig. 4. Irrespective of system size, we find that the success probability of achieving cooling saturates to a nonvanishing value, thereby ensuring the usefulness of this procedure. All the axes are dimensionless.

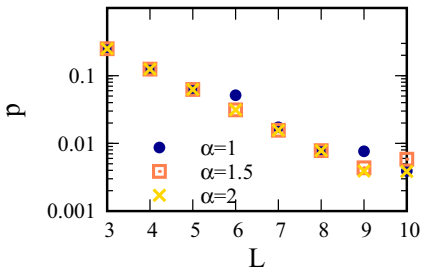

FIG. 8. Probability in log scale (ordinate) vs system size (abscissa). Circles, squares, and crosses represent different variable ranges of interactions. The plot depicts that p decreases with the increase of L. However, it is independent of the falloff rate of interactions α. All other specifications such as initial state and evolution operators are the same as in Figs. 4 and 5. Both axes are dimensionless.

In addition, we also examine the success probability of obtaining the measured qubit in the corresponding ground state after completion of each round. From Fig. 7, it is clear that increasing system size decreases the success probability monotonically for a moderate N. It is also independent of the range of interactions. Nonetheless, the success probability saturates with an increasing number of measurements, thereby establishing the usefulness of this protocol. With L, the success probability follows a scaling law which we will discuss below.

A. Scaling

Intuitively, in a measurement-based protocol, the success probability of finding the measured qubit in its corresponding ground state decreases with the increase in the number of measurements. However, we find that p_N first decreases and finally saturates after a certain value of N, as seen in Fig. 7. When the fidelities of all the individual unmeasured qubits approach the maximum fidelity i.e., $\mathcal{F} = 1$, after some steps N, we observe that the corresponding probability follows a scaling law with the system size L, given as

$$p = \left(\tfrac{1}{2}\right)^{L-1}, \tag{17}$$

which is independent of all the parameter values and the number of measurements. L is the total number of spin-$\frac{1}{2}$ particles in the spin chain. On the other hand, no such general relationship between the fidelity of the individual qubits and the system size is observed. Numerically, the scaling law of p for different values of α is depicted in Fig. 8, which is in good agreement with the expression in Eq. (17).

B. Dependence of initial temperature

Up to now, we have considered scenarios where the unmeasured qubits are prepared in maximally mixed states, i.e., thermal states with $\beta = 0$. Let us deal with the situation where the unmeasured initial states are thermal states with a moderate temperature. Such an analysis can reveal the dependence of the initial temperatures of unmeasured subsystems on the phenomenon of refrigeration.

The minimum number of measurements required to attain the ground state of all the individual qubits decreases with the increment of inverse temperature of the initial states, i.e., with the decrease in temperature, provided the involved system parameters are chosen appropriately. This behavior can be intuitively explained since the increasing value of β of an individual qubit makes the subsystem close to its respective ground state and hence fewer measurements are sufficient to cool down the system. However, the pattern of reduction of N with β is not *a priori* fixed. As observed in Fig. 9, the maximum number of measurements among all the unmeasured qubits is a linear function of β.

Let us define $N_\beta^{\alpha_i}$ as the number of steps required to reach the unit fidelity for all the unmeasured qubits. We observe that for moderate values of $\alpha > 1$, $N_\beta^{\alpha_i}$ scales linearly with β, and it increases monotonically with the system size. On the other hand, for $\alpha \leqslant 1$ and for a fixed L, $N_\beta^{\alpha_i}$ is much higher than the one with $\alpha > 1$, although the linear behavior of $N_\beta^{\alpha_i}$ with inverse temperature still holds. This show that although the

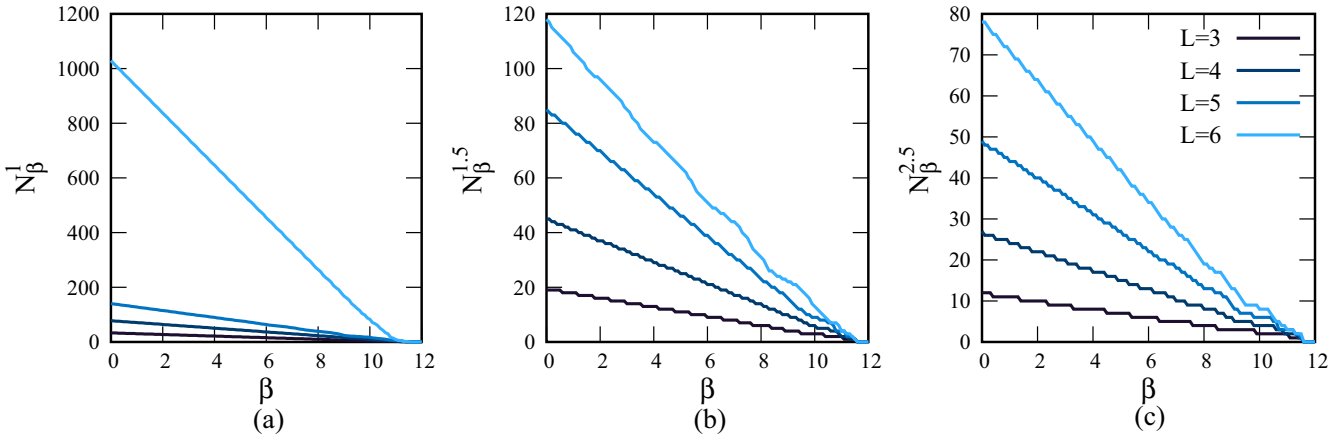

FIG. 9. Maximum number of measurements $N_\beta^{\alpha_i}$ required to obtain the unit fidelity in all subsystems (vertical axis) with the initial inverse temperature β (horizontal axis). Here (a) $\alpha_1 = 1$, (b) $\alpha_2 = 1.5$, and (c) $\alpha_3 = 2.5$. Different lines correspond to different system sizes L. The initial state is the thermal state with nonvanishing β. Dark to lighter shades occur with the increase of L. All other parameters are the same as in Fig. 4. All the axes are dimensionless.

interaction between subsystems which can create the correlation between the measured qubits is required to achieve cooling, the role of interaction in cooling is not ubiquitous. Precisely, for a fixed value of β, we find that

$$N_\beta^{\alpha_1} < N_\beta^{\alpha_2} < \cdots,$$

where $\alpha_1 > \alpha_2 > \cdots$. This indicates that irrespective of the temperature of the initial state, the range of interactions and interaction strength both have important roles to play in refrigeration.

V. SPATIAL POSITION OF MEASURED QUBITS VERSUS THE ENTANGLEMENT DISTRIBUTION OF UNMEASURED QUBITS

Due to the repeated measurements on the accessible qubit located on the boundary of the spin chain, by evolving the entire system according to the interacting Hamiltonian, we have already shown that the local energy of the rest of the system can be minimized provided suitable parameters are chosen. Removing the constraint on the position of the measured qubit, we explore here the situation in which the measurement can be carried out on any arbitrary qubit placed at an arbitrary position in a 1D array. Specifically, once the position of the measured qubit is fixed, in all the rounds of the protocol that particular qubit acts as the *measured qubit*. Interestingly, we find a notable difference between this and the previous scenario.

A refrigerator is built with L spin-$\frac{1}{2}$ particles arranged in a liner chain with the initial state

$$\rho(0) = |\mathcal{G}_{A_r^M}\rangle\langle\mathcal{G}_{A_r^M}| \bigotimes \rho_{\text{in}}^{L-1}, \tag{18}$$

where ρ_{in}^{L-1} is the thermal state of the individual local Hamiltonian H_{A_i} with $\omega_{A_i} = 1$ and $\beta = 0$. Here the site on which the measurement is performed is taken to be A_r^M. After the evolution according to H_{ev} and the outcome $|\mathcal{G}_{A_r^M}\rangle$, the output state after N rounds becomes

$$\begin{aligned}\rho(t) = {} & x_1|0\cdots10\cdots\rangle\langle0\cdots10\cdots0| \\ & + x_2 P_2\left[\sum a_r^1 \mathcal{P}[0\cdots11\cdots0]\right] \\ & + x_3 P_3\left[\sum a_r^2 \mathcal{P}[0\cdots111\cdots0]\right] + \cdots \\ & + x_L|111\cdots1\rangle\langle11\cdots1|,\end{aligned} \tag{19}$$

where $\mathcal{P}[0\cdots110\cdots0]$ denotes the permutation operator which permutes $(L-1)$ number of $|1\rangle$ states in all the L positions, keeping $|1\rangle$ fixed to the position A_r^M, on which the measurement is performed. The position of $|1\rangle$ in the first term is at the A_r^M position; in other terms, P_i's denote the projectors, and subscripts denote the number of $|1\rangle$ states present in the projector. The coefficients x_i and a_r^ks are functions of the system parameters.

Even vs odd. When the total number of qubits in the array of the spin chain is even, repeated measurements on a single qubit project all the subsystems into the corresponding ground state of the individual qubit (in most even cases).

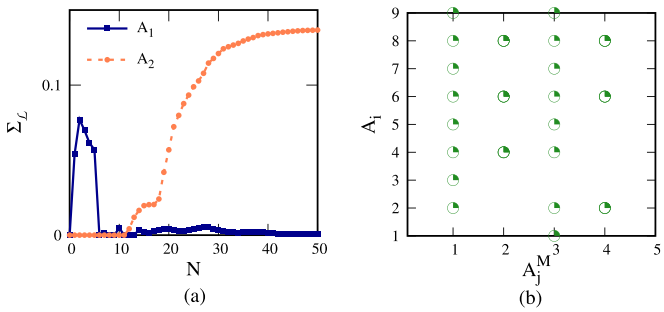

FIG. 10. Distribution of entanglement of unmeasured qubits and the role of position in a measured qubit. (a) Distribution of entanglement $\Sigma_{\mathcal{L}}$ defined in Eq. (20) (ordinate) vs N (abscissa). Squares represent the scenario in which the measurement is performed on the first qubit of a chain consisting of nine qubits, while circles correspond to the refrigerator in which the second qubit is measured. In the former scenario, the nodal site is taken to be the second qubit, and in the latter case, it is the first qubit. (b) The position of an unmeasured qubitA_i (ordinate) in a spin chain that reaches unit fidelity vs the position of a qubit on which the measurement is performed A_j^M (abscissa). Here $L = 9$. The parameters are the same as in Fig. 4. All the axes are dimensionless.

That is not the case when L is odd. Precisely, it is not always possible to cool down all the unmeasured qubits by measuring on an arbitrary qubit for odd values of L, irrespective of the number of rounds; that is, the maximum fidelity in this case saturates to a nonunit fidelity after N rounds of the protocol. The behavior is also independent of the choice of the involved system parameters. Specifically, we find that for odd L, if we measure on the qubits which are located in the odd positions, it is indeed possible to cool down all the qubits individually, while if we measure on the qubits belonging to the even sites of the spin chain, only the unmeasured qubits of the even sites attain their respective ground states (see Fig. 10). More interestingly, we report that it is impossible to cool down any qubit of the spin chain if the outcome of the qubit at position $\lfloor\frac{L}{2}\rfloor + 1$ is the ground state of the local Hamiltonian when L is odd [see Fig. 10(b) for $A_j^M = 5$]. We will now argue that the odd-even dichotomy can be qualitatively explained by the pattern of entanglement established between the unmeasured qubits after the unitary evolution of the entire system and each round of measurements.

Distribution of entanglement. Let the number of sites of the spin chain be L and the measurement be performed on A_r^M. We compute the distribution of entanglement [48,49] as

$$\Sigma_{\mathcal{L}} = \sum_{\substack{i=1 \\ i\neq r}}^{L} \mathcal{E}(\varrho_{A_{r-1}A_i}), \tag{20}$$

where $\mathcal{E}$ is any entanglement measure. In our case, we compute logarithmic negativity [51,52] as an entanglement measure, and the corresponding quantity is denoted by $\Sigma_{\mathcal{L}}$. Here A_{r-1} is the nearest-neighbor site of the measured qubit, which is taken to be a nodal site. In a similar argument, A_{r+1} can also be taken to be the nodal party, which is the case when the first qubit is measured.

For odd L, when the measurement is performed on the odd qubits, $\Sigma_{\mathcal{L}}$ decreases with an increasing number of measurements, thereby demonstrating the action of a refrigerator, while $\Sigma_{\mathcal{L}}$ saturates with N when the measurements are performed on the even qubits, implying that not all the qubits attain their corresponding ground states. When all the subsystems reach their ground states, the final state becomes fully separable, and hence, $\Sigma_{\mathcal{L}} = 0$ in the former case, which is not true for the latter case. Figure 10(a) clearly mimics this behavior of a chain with nine sites.

VI. CONCLUSION

The idea of miniaturization of devices has revolutionized the field of technology, naturally surpassing classical technology based on classical physics. Therefore, it is a great time to go beyond it and formulate new sketches of old machines on the breadboard of quantum systems. Due to rapid experimental advancements in the quantum domain, one can expect to implement these devices not only in laboratories but also on an industrial scale.

In summary, we proposed a quantum refrigerator model based on multiple measurement schemes. Specifically, all the subsystems are initially prepared in thermal states except the one which is to be measured in the ground state of a local magnetic field after a certain interval of time. During the dynamics, the system evolves according to an interacting Hamiltonian, a one-dimensional XY spin chain with long-range interaction present between the subsystems in the presence of a transverse magnetic field, and then a measurement is performed at a fixed site. We analyzed the final state of the unmeasured qubits as a consequence of these repeated evolutions and measurements. We observed that the projection of a prefixed qubit to its ground state can project other unmeasured qubits to their minimum energy states, thereby exhibiting the phenomenon of cooling. In contrast to previous designs of a quantum refrigerator in which a single system was considered as a target system to cool down, in the current proposal, we can cool more than one subsystem by measuring only a single qubit, showing scalability of the cooling mechanism.

The previous understanding of a quantum refrigerator was based on a master-equation approach where each qubit or part of the system is attached to the environment and a target system is taken to be refrigerated. Our approach differs from the previous proposals in the sense that part of the spin models can be thought of as an environment and the rest can act as a refrigerator in which the accessible qubits are used to perform repeated measurements. Moreover, we showed that by wisely choosing system parameters, an efficient quantum refrigerator can be constructed in which fewer measurements are required and it can be realized with a nonvanishing success probability. We also found that the position of a qubit in an array of spin-$\frac{1}{2}$ particles chosen for measurement can dictate the amount of cooling, quantified via the fidelity between the resulting state and the ground state of the local Hamiltonian and the success probability. We believe that the design of a refrigerator based on measurements may provide a different framework to build quantum thermal machines.

ACKNOWLEDGMENTS

We acknowledge the support from the Interdisciplinary Cyber Physical Systems (ICPS) program of the Department of Science and Technology (DST), India, Grant No. DST/ICPS/QuST/Theme- 1/2019/23. We acknowledge the use of QICLIB [53] a modern C++ library for general-purpose quantum information processing and quantum computing, and the cluster computing facility at the Harish-Chandra Research Institute.

[1] G. Gemmer, M. Michel, and G. Mahler, *Quantum Thermodynamics* (Springer, New York, 2004)
[2] F. Binder, A. Correa, L, J. Andres, and G. Adesso, *Thermodynamics in the Quantum Regime,* Fundamental Theories of Physics (Springer, Cham, Switzerland, 2018).
[3] J. Lekscha, H. Wilming, J. Eisert, and R. Gallego, Phys. Rev. E **97**, 022142 (2018).
[4] S. Deffner and S. Campbell, *Quantum Thermodynamics* (Morgan and Claypool Publishers, San Rafael, CA, USA, 2019).
[5] R. Alicki and M. Fannes, Phys. Rev. E **87**, 042123 (2013).
[6] K. Joulain, J. Drevillon, Y. Ezzahri, and J. Ordonez-Miranda, Phys. Rev. Lett. **116**, 200601 (2016).
[7] J. Ordonez-Miranda, Y. Ezzahri, and K. Joulain, Phys. Rev. E **95**, 022128 (2017).
[8] N. Linden, S. Popescu, and P. Skrzypczyk, Phys. Rev. Lett. **105**, 130401 (2010).
[9] A. E. Allahverdyan, K. Hovhannisyan, and G. Mahler, Phys. Rev. E **81**, 051129 (2010).
[10] A. Levy and R. Kosloff, Phys. Rev. Lett. **108**, 070604 (2012).
[11] A. Hewgill, J. O. González, J. P. Palao, D. Alonso, A. Ferraro, and G. De Chiara, Phys. Rev. E **101**, 012109 (2020).
[12] D. Ferraro, M. Campisi, G. M. Andolina, V. Pellegrini, and M. Polini, Phys. Rev. Lett. **120**, 117702 (2018).
[13] L. A. Correa, Phys. Rev. E **89**, 042128 (2014).
[14] J. Wang, Y. Lai, Z. Ye, J. He, Y. Ma, and Q. Liao, Phys. Rev. E **91**, 050102(R) (2015).
[15] R. Silva, G. Manzano, P. Skrzypczyk, and N. Brunner, Phys. Rev. E **94**, 032120 (2016).
[16] T. K. Konar, S. Ghosh, A. K. Pal, and A. Sen(De), Beyond qubits: Building quantum refrigerators in higher dimensions, arXiv:2112.13765.
[17] Y. Li, L.-A. Wu, Y.-D. Wang, and L.-P. Yang, Phys. Rev. B **84**, 094502 (2011).
[18] T. K. Konar, S. Ghosh, A. K. Pal, and A. Sen(De), Phys. Rev. A **105**, 022214 (2022).
[19] L.-M. Duan, E. Demler, and M. D. Lukin, Phys. Rev. Lett. **91**, 090402 (2003).
[20] E. Köse, S. Çakmak, A. Gençten, I. K. Kominis, and O. E. Müstecaplıoğlu, Phys. Rev. E **100**, 012109 (2019).
[21] G. Maslennikov, S. Ding, R. Hablützel, J. Gan, A. Roulet, S. Nimmrichter, J. Dai, V. Scarani, and D. Matsukevich, Nat. Commun. **10**, 202 (2019).

[22] M. T. Mitchison, M. Huber, J. Prior, M. P. Woods, and M. B. Plenio, Quantum Sci. Technol. **1**, 015001 (2016).
[23] S. K. Manikandan, F. Giazotto, and A. N. Jordan, Phys. Rev. Applied **11**, 054034 (2019).
[24] M. J. Henrich, G. Mahler, and M. Michel, Phys. Rev. E **75**, 051118 (2007).
[25] M. Huber, M. Perarnau-Llobet, K. V. Hovhannisyan, P. Skrzypczyk, C. Klöckl, N. Brunner, and A. Acín, New J. Phys. **17**, 065008 (2015).
[26] S. Das, A. Misra, A. K. Pal, A. Sen(De), and U. Sen, Europhys. Lett. **125**, 20007 (2019).
[27] H.-P. Breuer and F. Petruccione, *The Theory of Open Quantum Systems* (Oxford University Press, Oxford, 2007).
[28] F. Tonner and G. Mahler, Phys. Rev. E **72**, 066118 (2005).
[29] B. Bhandari and A. N. Jordan, Phys. Rev. B **104**, 075442 (2021).
[30] L. A. Correa, J. P. Palao, G. Adesso, and D. Alonso, Phys. Rev. E **87**, 042131 (2013).
[31] W. Niedenzu, V. Mukherjee, A. Ghosh, A. G. Kofman, and G. Kurizki, Nat. Commun. **9**, 165 (2018).
[32] G. D. Chiara, G. Landi, A. Hewgill, B. Reid, A. Ferraro, A. J. Roncaglia, and M. Antezza, New J. Phys. **20**, 113024 (2018).
[33] R. Silva, P. Skrzypczyk, and N. Brunner, Phys. Rev. E **92**, 012136 (2015).
[34] A. Rivas and S. F. Huelga, *Open Quantum Systems: An Introduction*, Springer Briefs in Physics (Springer, Berlin, Heidelberg, 2012).
[35] H. Nakazato, T. Takazawa, and K. Yuasa, Phys. Rev. Lett. **90**, 060401 (2003).
[36] H. Nakazato, M. Unoki, and K. Yuasa, Phys. Rev. A **70**, 012303 (2004).
[37] D. Burgarth and V. Giovannetti, Phys. Rev. A **76**, 062307 (2007).
[38] D. Burgarth and V. Giovannetti, arXiv:0710.0302.
[39] P. V. Pyshkin, D.-W. Luo, J. Q. You, and L.-A. Wu, Phys. Rev. A **93**, 032120 (2016).
[40] V. Montenegro, R. Coto, V. Eremeev, and M. Orszag, Phys. Rev. A **98**, 053837 (2018).
[41] R. Puebla, O. Abah, and M. Paternostro, Phys. Rev. B **101**, 245410 (2020).
[42] J.-M. Zhang, J. Jing, L.-A. Wu, L.-G. Wang, and S.-Y. Zhu, Phys. Rev. A **100**, 022107 (2019).
[43] J.-s. Yan and J. Jing, Phys. Rev. A **104**, 063105 (2021).
[44] J.-S. Yan and J. Jing, Phys. Rev. A **105**, 052607 (2022).
[45] L.-A. Wu, D. A. Lidar, and S. Schneider, Phys. Rev. A **70**, 032322 (2004).
[46] N. Qiu, S.-c. Wang, L. C. Kwek, and X.-B. Wang, Phys. Rev. A **86**, 012313 (2012).
[47] B. Misra and E. C. G. Sudarshan, J. Math. Phys. **18**, 756 (1977).
[48] V. Coffman, J. Kundu, and W. K. Wootters, Phys. Rev. A **61**, 052306 (2000).
[49] H. S. Dhar, A. K. Pal, D. Rakshit, A. Sen(De), and U. Sen, in *Lectures on General Quantum Correlations and Their Applications*, edited by F. F. Fanchini, D. d. O. Soares Pinto, and G. Adesso (Springer, Cham, 2017), pp. 23–64.
[50] R. Horodecki, P. Horodecki, M. Horodecki, and K. Horodecki, Rev. Mod. Phys. **81**, 865 (2009).
[51] G. Vidal and R. F. Werner, Phys. Rev. A **65**, 032314 (2002).
[52] M. B. Plenio, Phys. Rev. Lett. **95**, 090503 (2005).
[53] QICLIB, https://titaschanda.github.io/QIClib.